PHYSICAL REVIEW D **83,** 032003 (2011)

Study of $a_0^0(980) - f_0(980)$ mixing

M. Ablikim,[1] M. N. Achasov,[5] L. An,[9] Q. An,[36] Z. H. An,[1] J. Z. Bai,[1] R. Baldini,[17] Y. Ban,[23] J. Becker,[2] N. Berger,[1] M. Bertani,[17] J. M. Bian,[1] I. Boyko,[15] R. A. Briere,[3] V. Bytev,[15] X. Cai,[1] G. F. Cao,[1] X. X. Cao,[1] J. F. Chang,[1] G. Chelkov,[15,*] G. Chen,[1] H. S. Chen,[1] J. C. Chen,[1] M. L. Chen,[1] S. J. Chen,[21] Y. Chen,[1] Y. B. Chen,[1] H. P. Cheng,[11] Y. P. Chu,[1] D. Cronin-Hennessy,[35] H. L. Dai,[1] J. P. Dai,[1] D. Dedovich,[15] Z. Y. Deng,[1] I. Denysenko,[15,†] M. Destefanis,[38] Y. Ding,[19] L. Y. Dong,[1] M. Y. Dong,[1] S. X. Du,[42] M. Y. Duan,[26] R. R. Fan,[1] J. Fang,[1] S. S. Fang,[1] C. Q. Feng,[36] C. D. Fu,[1] J. L. Fu,[21] Y. Gao,[32] C. Geng,[36] K. Goetzen,[7] W. X. Gong,[1] M. Greco,[38] S. Grishin,[15] M. H. Gu,[1] Y. T. Gu,[9] Y. H. Guan,[6] A. Q. Guo,[22] L. B. Guo,[20] Y. P. Guo,[22] X. Q. Hao,[1] F. A. Harris,[34] K. L. He,[1] M. He,[1] Z. Y. He,[22] Y. K. Heng,[1] Z. L. Hou,[1] H. M. Hu,[1] J. F. Hu,[6] T. Hu,[1] B. Huang,[1] G. M. Huang,[12] J. S. Huang,[10] X. T. Huang,[25] Y. P. Huang,[1] T. Hussain,[37] C. S. Ji,[36] Q. Ji,[1] X. B. Ji,[1] X. L. Ji,[1] L. K. Jia,[1] L. L. Jiang,[1] X. S. Jiang,[1] J. B. Jiao,[25] Z. Jiao,[11] D. P. Jin,[1] S. Jin,[1] F. F. Jing,[32] M. Kavatsyuk,[16] S. Komamiya,[31] W. Kuehn,[33] J. S. Lange,[33] J. K. C. Leung,[30] Cheng Li,[36] Cui Li,[36] D. M. Li,[42] F. Li,[1] G. Li,[1] H. B. Li,[1] J. C. Li,[1] Lei Li,[1] N. B. Li,[20] Q. J. Li,[1] W. D. Li,[1] W. G. Li,[1] X. L. Li,[25] X. N. Li,[1] X. Q. Li,[22] X. R. Li,[1] Z. B. Li,[28] H. Liang,[36] Y. F. Liang,[27] Y. T. Liang,[33] G. R. Liao,[8] X. T. Liao,[1] B. J. Liu,[29] B. J. Liu,[30] C. L. Liu,[3] C. X. Liu,[1] C. Y. Liu,[1] F. H. Liu,[26] Fang Liu,[1] Feng Liu,[12] G. C. Liu,[1] H. Liu,[1] H. B. Liu,[6] H. M. Liu,[1] H. W. Liu,[1] J. P. Liu,[40] K. Liu,[23] K. Y. Liu,[19] Q. Liu,[34] S. B. Liu,[36] X. Liu,[18] X. H. Liu,[1] Y. B. Liu,[22] Y. W. Liu,[36] Yong Liu,[1] Z. A. Liu,[1] Z. Q. Liu,[1] H. Loehner,[16] G. R. Lu,[10] H. J. Lu,[11] J. G. Lu,[1] Q. W. Lu,[26] X. R. Lu,[6] Y. P. Lu,[1] C. L. Luo,[20] M. X. Luo,[41] T. Luo,[1] X. L. Luo,[1] C. L. Ma,[6] F. C. Ma,[19] H. L. Ma,[1] Q. M. Ma,[1] T. Ma,[1] X. Ma,[1] X. Y. Ma,[1] M. Maggiora,[38] Q. A. Malik,[37] H. Mao,[1] Y. J. Mao,[23] Z. P. Mao,[1] J. G. Messchendorp,[16] J. Min,[1] R. E. Mitchell,[14] X. H. Mo,[1] N. Yu. Muchnoi,[5] Y. Nefedov,[15] Z. Ning,[1] S. L. Olsen,[24] Q. Ouyang,[1] S. Pacetti,[17] M. Pelizaeus,[34] K. Peters,[7] J. L. Ping,[20] R. G. Ping,[1] R. Poling,[35] C. S. J. Pun,[30] M. Qi,[21] S. Qian,[1] C. F. Qiao,[6] X. S. Qin,[1] J. F. Qiu,[1] K. H. Rashid,[37] G. Rong,[1] X. D. Ruan,[9] A. Sarantsev,[15,‡] J. Schulze,[2] M. Shao,[36] C. P. Shen,[34] X. Y. Shen,[1] H. Y. Sheng,[1] M. R. Shepherd,[14] X. Y. Song,[1] S. Sonoda,[31] S. Spataro,[38] B. Spruck,[33] D. H. Sun,[1] G. X. Sun,[1] J. F. Sun,[10] S. S. Sun,[1] X. D. Sun,[1] Y. J. Sun,[36] Y. Z. Sun,[1] Z. J. Sun,[1] Z. T. Sun,[36] C. J. Tang,[27] X. Tang,[1] X. F. Tang,[8] H. L. Tian,[1] D. Toth,[35] G. S. Varner,[34] X. Wan,[1] B. Q. Wang,[23] K. Wang,[1] L. L. Wang,[4] L. S. Wang,[1] M. Wang,[25] P. Wang,[1] P. L. Wang,[1] Q. Wang,[1] S. G. Wang,[23] X. L. Wang,[36] Y. D. Wang,[36] Y. F. Wang,[1] Y. Q. Wang,[25] Z. Wang,[1] Z. G. Wang,[1] Z. Y. Wang,[1] D. H. Wei,[8] S. P. Wen,[1] U. Wiedner,[2] L. H. Wu,[1] N. Wu,[1] W. Wu,[19] Z. Wu,[1] Z. J. Xiao,[20] Y. G. Xie,[1] G. F. Xu,[1] G. M. Xu,[23] H. Xu,[1] Y. Xu,[22] Z. R. Xu,[36] Z. Z. Xu,[36] Z. Xue,[1] L. Yan,[36] W. B. Yan,[36] Y. H. Yan,[13] H. X. Yang,[1] M. Yang,[1] T. Yang,[9] Y. Yang,[12] Y. X. Yang,[8] M. Ye,[1] M. H. Ye,[4] B. X. Yu,[1] C. X. Yu,[22] L. Yu,[12] C. Z. Yuan,[1] W. L. Yuan,[20] Y. Yuan,[1] A. A. Zafar,[37] A. Zallo,[17] Y. Zeng,[13] B. X. Zhang,[1] B. Y. Zhang,[1] C. C. Zhang,[1] D. H. Zhang,[1] H. H. Zhang,[28] H. Y. Zhang,[1] J. Zhang,[20] J. W. Zhang,[1] J. Y. Zhang,[1] J. Z. Zhang,[1] L. Zhang,[21] S. H. Zhang,[1] T. R. Zhang,[20] X. J. Zhang,[1] X. Y. Zhang,[25] Y. Zhang,[1] Y. H. Zhang,[1] Z. P. Zhang,[36] Z. Y. Zhang,[40] G. Zhao,[1] H. S. Zhao,[1] Jiawei Zhao,[36] Jingwei Zhao,[1] Lei Zhao,[36] Ling Zhao,[1] M. G. Zhao,[22] Q. Zhao,[1] S. J. Zhao,[42] T. C. Zhao,[39] X. H. Zhao,[21] Y. B. Zhao,[1] Z. G. Zhao,[36] Z. L. Zhao,[9] A. Zhemchugov,[15,*] B. Zheng,[1] J. P. Zheng,[1] Y. H. Zheng,[6] Z. P. Zheng,[1] B. Zhong,[1] J. Zhong,[2] L. Zhong,[32] L. Zhou,[1] X. K. Zhou,[6] X. R. Zhou,[36] C. Zhu,[1] K. Zhu,[1] K. J. Zhu,[1] S. H. Zhu,[1] X. L. Zhu,[32] X. W. Zhu,[1] Y. S. Zhu,[1] Z. A. Zhu,[1] J. Zhuang,[1] B. S. Zou,[1] J. H. Zou,[1] J. X. Zuo,[1] and P. Zweber[3]

(BES III Collaboration)

[1]*Institute of High Energy Physics, Beijing 100049, People's Republic of China*
[2]*Bochum Ruhr-University, 44780 Bochum, Germany*
[3]*Carnegie Mellon University, Pittsburgh, Pennsylvania 15213, USA*
[4]*China Center of Advanced Science and Technology, Beijing 100190, People's Republic of China*
[5]*G. I. Budker Institute of Nuclear Physics SB RAS (BINP), Novosibirsk 630090, Russia*
[6]*Graduate University of Chinese Academy of Sciences, Beijing 100049, People's Republic of China*
[7]*GSI Helmholtzcentre for Heavy Ion Research GmbH, D-64291 Darmstadt, Germany*
[8]*Guangxi Normal University, Guilin 541004, People's Republic of China*
[9]*Guangxi University, Naning 530004, People's Republic of China*
[10]*Henan Normal University, Xinxiang 453007, People's Republic of China*
[11]*Huangshan College, Huangshan 245000, People's Republic of China*
[12]*Huazhong Normal University, Wuhan 430079, People's Republic of China*
[13]*Hunan University, Changsha 410082, People's Republic of China*
[14]*Indiana University, Bloomington, Indiana 47405, USA*
[15]*Joint Institute for Nuclear Research, 141980 Dubna, Russia*

[16]KVI/University of Groningen, 9747 AA Groningen, The Netherlands
[17]Laboratori Nazionali di Frascati - INFN, 00044 Frascati, Italy
[18]Lanzhou University, Lanzhou 730000, People's Republic of China
[19]Liaoning University, Shenyang 110036, People's Republic of China
[20]Nanjing Normal University, Nanjing 210046, People's Republic of China
[21]Nanjing University, Nanjing 210093, People's Republic of China
[22]Nankai University, Tianjin 300071, People's Republic of China
[23]Peking University, Beijing 100871, People's Republic of China
[24]Seoul National University, Seoul, 151-747 Korea
[25]Shandong University, Jinan 250100, People's Republic of China
[26]Shanxi University, Taiyuan 030006, People's Republic of China
[27]Sichuan University, Chengdu 610064, People's Republic of China
[28]Sun Yat-Sen University, Guangzhou 510275, People's Republic of China
[29]The Chinese University of Hong Kong, Shatin, N.T., Hong Kong
[30]The University of Hong Kong, Pokfulam, Hong Kong
[31]The University of Tokyo, Tokyo 113-0033, Japan
[32]Tsinghua University, Beijing 100084, People's Republic of China
[33]Universitaet Giessen, 35392 Giessen, Germany
[34]University of Hawaii, Honolulu, Hawaii 96822, USA
[35]University of Minnesota, Minneapolis, Minnesota 55455, USA
[36]University of Science and Technology of China, Hefei 230026, People's Republic of China
[37]University of the Punjab, Lahore-54590, Pakistan
[38]University of Turin and INFN, Turin, Italy
[39]University of Washington, Seattle, Washington 98195, USA
[40]Wuhan University, Wuhan 430072, People's Republic of China
[41]Zhejiang University, Hangzhou 310027, People's Republic of China
[42]Zhengzhou University, Zhengzhou 450001, People's Republic of China
(Received 23 December 2010; published 3 February 2011)

Using samples of 2.25×10^8 J/ψ events and 1.06×10^8 ψ' events collected with the BES III detector, we study the $f_0(980) \to a_0^0(980)$ and $a_0^0(980) \to f_0(980)$ transitions in the processes $J/\psi \to \phi f_0(980) \to \phi a_0^0(980)$ and $\chi_{c1} \to \pi^0 a_0^0(980) \to \pi^0 f_0(980)$, respectively. Evidence for $f_0(980) \to a_0^0(980)$ is found with a significance of 3.4σ, while in the case of $a_0^0(980) \to f_0(980)$ transition, the significance is 1.9σ. Measurements and upper limits of both branching ratios and mixing intensities are determined.

DOI: 10.1103/PhysRevD.83.032003 PACS numbers: 14.40.Df, 25.75.Gz

I. INTRODUCTION

The nature of the scalar mesons $a_0(980)$ and $f_0(980)$ has been a hot topic in light hadron physics for many years. These two states, with similar masses but different decay modes, are difficult to accommodate in the constituent quark-antiquark scenario. Tremendous efforts in both experiment and theory have been made in order to understand them. Suggestions for their being exotic candidates, such as tetraquark states, hybrids, or $K\bar{K}$ molecules, can be found in the literature [1–6].

The possibility of mixing between $a_0^0(980)$ and $f_0(980)$ was suggested long ago, and its measurement will shed light on the nature of these two resonances [7–14]. In particular, the leading contribution to the isospin-violating mixing transition amplitudes for $f_0(980) \to a_0^0(980)$ and $a_0^0(980) \to f_0(980)$ is shown to be dominated by the difference of the unitarity cut which arises from the mass difference between the charged and neutral $K\bar{K}$ pairs. As a consequence, a narrow peak of about 8 MeV/c^2 is predicted between the charged and neutral $K\bar{K}$ thresholds [8,13,14].

The mixing amplitudes strongly depend on the couplings of $a_0^0(980)$ and $f_0(980)$ to $K\bar{K}$, and to probe the properties of these two scalar states, precise measurements of the mixing transitions are very important. Two kinds of mixing intensities, i.e. ξ_{fa} and ξ_{af} for the $f_0(980) \to a_0^0(980)$ and $a_0^0(980) \to f_0(980)$ transitions, respectively, can be defined and are accessible to measurement in charmonium decays [13,14]:

$$\xi_{fa} \equiv \frac{\mathrm{Br}(J/\psi \to \phi f_0(980) \to \phi a_0^0(980) \to \phi \eta \pi^0)}{\mathrm{Br}(J/\psi \to \phi f_0(980) \to \phi \pi \pi)}$$

and

$$\xi_{af} \equiv \frac{\mathrm{Br}(\chi_{c1} \to \pi^0 a_0^0(980) \to \pi^0 f_0(980) \to \pi^0 \pi^+ \pi^-)}{\mathrm{Br}(\chi_{c1} \to \pi^0 a_0^0(980) \to \pi^0 \pi^0 \eta)}.$$

*Also at the Moscow Institute of Physics and Technology, Moscow, Russia.
†On leave from the Bogolyubov Institute for Theoretical Physics, Kiev, Ukraine.
‡Also at the PNPI, Gatchina, Russia.

Using samples of $2.25 \times 10^8 J/\psi$ events [15] and $1.06 \times 10^8 \psi'$ events [16] collected with the BES III detector in 2009, we perform direct measurements of the $a_0^0(980) - f_0(980)$ mixing intensities via the processes $J/\psi \to \phi f_0(980) \to \phi a_0^0(980) \to \phi\eta\pi^0$ and $\chi_{c1} \to \pi^0 a_0^0(980) \to \pi^0 f_0(980) \to \pi^0\pi^+\pi^-$.

II. DETECTOR AND MONTE CARLO SIMULATION

BEPC II is a double-ring e^+e^- collider designed to provide a peak luminosity of 10^{33} cm^{-2} s^{-1} at a beam current of 0.93 A. The BES III detector has a geometrical acceptance of 93% of 4π and has four main components: (1) A small-cell, helium-based (40% He, 60% C_3H_8) main drift chamber with 43 layers providing an average single-hit resolution of 135 μm, charged-particle momentum resolution in a 1 T magnetic field of 0.5% at 1 GeV/c, and the dE/dx resolution that is better than 6%. (2) An electromagnetic calorimeter (EMC) consisting of 6240 CsI (Tl) crystals in a cylindrical structure (barrel) and two end caps. The energy resolution at 1.0 GeV/c is 2.5% (5%) in the barrel (end caps), and the position resolution is 6 mm (9 mm) in the barrel (end caps). (3) A time-of-flight system constructed of 5-cm-thick plastic scintillators, with 176 detectors of 2.4 m length in two layers in the barrel and 96 fan-shaped detectors in the end caps. The barrel (end cap) time resolution of 80 ps (110 ps) provides $2\sigma K/\pi$ separation for momenta up to $\sim$1.0 GeV/c. (4) The muon system consists of 1000 m^2 of resistive plate chambers in nine barrel and eight end cap layers and provides 2 cm position resolution.

The efficiency for $J/\psi \to \phi f_0(980) \to \phi a_0^0(980) \to \phi\eta\pi^0$ is estimated using a Monte Carlo (MC) simulation of $J/\psi \to \phi S$, where S is the mixing signal represented by a narrow scalar Breit-Wigner uniformly decaying to $\eta\pi^0$. The mass of the mixing signal is set to be 991.3 MeV/c^2 [the center of $(m_{K^+} + m_{K^-})$ and $(m_{K^0} + m_{\bar{K}^0})$ [17]], and the width of the mixing signal is set to be 8 MeV/c^2. The efficiency for $\psi' \to \gamma\chi_{c1} \to \gamma\pi^0 a_0^0(980) \to \gamma\pi^0 f_0(980) \to \gamma\pi^0\pi^+\pi^-$ is estimated using a Monte Carlo simulation of $\psi' \to \gamma\chi_{c1} \to \gamma\pi^0 S$, where S is the mixing signal with parameters as above, and decays into $\pi^+\pi^-$ isotropically.

III. EVENT SELECTION

Tracks of charged particles in BES III are reconstructed from main drift chamber hits. We select tracks within $\pm$20 cm of the interaction point in the beam direction and within 2 cm in the plane perpendicular to the beam. The time-of-flight and dE/dx information are combined to form particle identification (PID) confidence levels for the π, K, and p hypotheses; each track is assigned to the particle type that corresponds to the hypothesis with the highest confidence level.

Photon candidates are reconstructed by clustering EMC crystal energies. Efficiency and energy resolution are improved by including energy deposits in nearby time-of-flight counters. The minimum energy is 25 MeV for barrel showers ($|\cos\theta| < 0.80$) and 50 MeV for end cap showers ($0.86 < |\cos\theta| < 0.92$). To exclude showers from charged particles, the angle between the nearest charged track and the shower must be greater than 10°. EMC cluster timing requirements suppress electronic noise and energy deposits unrelated to the event.

The $\pi^0 \to \gamma\gamma$ and $\eta \to \gamma\gamma$ candidates are formed from pairs of photon candidates that are kinematically fit to the known resonance masses, and the χ^2 from the kinematic fit with 1 degree of freedom is required to be less than 25. The decay angle of a photon is the polar angle measured in the η or π^0 rest frame with respect to the η or π^0 direction in the J/ψ or ψ' rest frame. Real η and π^0 mesons decay isotropically, and their angular distributions are flat. However, the η and π^0 candidates which originate from a wrong photon combination do not have a flat distribution in this variable. To remove wrong photon combinations, the decay angle is required to satisfy $|\cos\theta_{\text{decay}}| < 0.95$.

IV. MEASUREMENT OF $J/\psi \to \phi f_0(980) \to \phi a_0^0(980) \to \phi\eta\pi^0$

Events with two oppositely charged tracks identified as kaons and at least one distinct π^0 candidate and η candidate are selected. A six-constraint kinematic fit (6C) is performed to the $J/\psi \to K^+K^-\eta\pi^0$ hypothesis (constraints are the 4-momentum of the J/ψ and the π^0 and η masses), and $\chi^2_{6C} < 60$ is required. If there is more than one combination, the combination with the smallest χ^2_{6C} is retained. The events are fitted to $J/\psi \to K^+K^-\eta\eta$ and $J/\psi \to K^+K^-\pi^0\pi^0$, and the probabilities are required to be less than that from the kinematic fit to the signal channel $J/\psi \to K^+K^-\eta\pi^0$. The K^+K^- invariant mass distribution of selected events is shown in Fig. 1(a), where a clear ϕ signal can be seen. The solid and dashed arrows show the signal and sideband regions, respectively.

Figure 1(b) shows the $\eta\pi^0$ invariant mass distribution recoiling against the ϕ signal ($|m_{K^+K^-} - 1.02| < 0.015$ GeV/c^2). A narrow structure appears around 980 MeV/c^2. The shaded histogram shows the $\eta\pi^0$ invariant mass of events recoiling against the ϕ sideband (1.065 GeV/$c^2 < M_{K^+K^-} <$ 1.095 GeV/c^2), and no sign of a peak near 980 MeV/c^2 is evident.

Exclusive MC samples of J/ψ decays which have similar final states are generated to check whether a peak near 980 MeV/c^2 can be produced in the $\eta\pi^0$ mass spectrum. The main backgrounds come from: (1) $J/\psi \to \phi\pi^0\pi^0$ via $f_0(980)$, $f_2(1270)$, or a phase space process; and (2) $J/\psi \to K^*\bar{K}\eta$ + c.c., $J/\psi \to K_2^*(1430)\bar{K}\eta$ + c.c., and $J/\psi \to \gamma f_2(1950) \to \gamma K^*\bar{K}^*$. The $\eta\pi^0$ invariant mass distribution from all these possible background

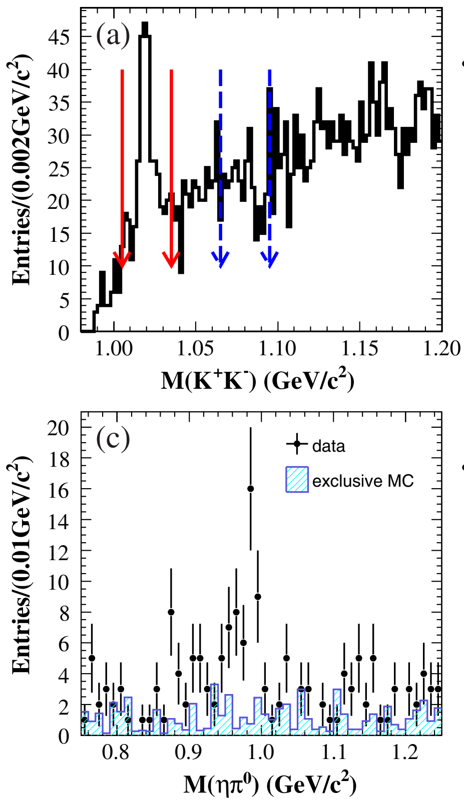

FIG. 1 (color online). (a) The invariant mass spectrum of K^+K^- in $J/\psi \to K^+K^-\eta\pi^0$. The solid arrows show the ϕ mass window. The dashed arrows show the ϕ sideband region used to estimate backgrounds. The $\eta\pi^0$ invariant mass of selected events is shown in (b)–(d). The dots with error bars show the mass spectrum of $M_{\eta\pi^0}$ recoiling against the ϕ. The shaded histogram is (b) recoiling against the ϕ sideband; (c) from exclusive MC; and (d) from inclusive MC.

channels is smooth, shown as the shaded region in Fig. 1(c), and will not affect the determination of the number of mixing events.

A MC sample of 2.0×10^8 inclusive J/ψ decay events is used to investigate other possible backgrounds too. The shaded histogram in Fig. 1(d) shows the $\eta\pi^0$ invariant mass distributions of events selected from the inclusive MC sample. In the 980 MeV$/c^2$ region, there is no peaking background.

An underlying process is from $J/\psi \to \phi a_0^0(980)$ via a γ^* or K^*K loops [13]. However, it will produce a much broader distribution (50–100 MeV$/c^2$) in the $\eta\pi^0$ mass spectrum than $f_0(980) \to a_0^0(980)$ mixing [13]. We estimate its contribution in the fit to the mass spectrum.

A simultaneous unbinned maximum likelihood fit to the $\eta\pi^0$ mass spectrums recoiling against the ϕ and the ϕ sideband is performed. In the signal region, the probability density function is composed of the mixing signal, represented by the shape extracted from MC simulation of a narrow Breit-Wigner, the $a_0^0(980)$ contribution from γ^* or K^*K loops represented by a Flatté formula,[1] and a 2nd order polynomial for the backgrounds. In the sideband region, the probability density function is a 2nd order polynomial only. The mass of the mixing signal is set to 991.3 MeV$/c^2$ [the center of $(m_{K^+} + m_{K^-})$ and $(m_{K^0} + m_{\bar{K}^0})$ [17]], and the width of the mixing signal is set to 8 MeV$/c^2$. The shape parameters of the background polynomials in the signal region and the sideband region are constrained to vary simultaneously in the fit. The normalization of each component is allowed to float. Figures 2(a) and 2(b) show the results of the simultaneous fit.

The fit yields $N(f_0 \to a_0^0) = 25.8 \pm 8.6$ events for the mixing signal and $N(a_0^0(980)) = 13.6 \pm 24.8$ events for the $a_0^0(980)$ contribution from γ^* or K^*K loops. Comparing with the fit result without the mixing signal, the change in $-lnL$ with $\Delta(\text{d.o.f.}) = 1$ is 5.90, corresponding to a statistical significance of 3.4σ. Comparing with the fit result without the $a_0^0(980)$ contribution from γ^* or K^*K loops, the change in $-lnL$ with $\Delta(\text{d.o.f.}) = 1$ is 0.14, corresponding to a statistical significance of 0.5σ. Using the Bayesian method, the upper limit for the number of mixing events is 37.5, and the upper limit of the number of $a_0^0(980)$ from γ^* or K^*K loops is 50.8 events at the 90% confidence level (C.L.). The results are listed in Table I.

The branching ratio of the mixing signal $J/\psi \to \phi f_0(980) \to \phi a_0^0(980) \to \phi\eta\pi^0$ is calculated as

[1]The Flatté formula is taken from Ref. [18]. The values of coupling constants and mass as used here are taken from the Crystal Barrel experiment results in Ref. [13,19].

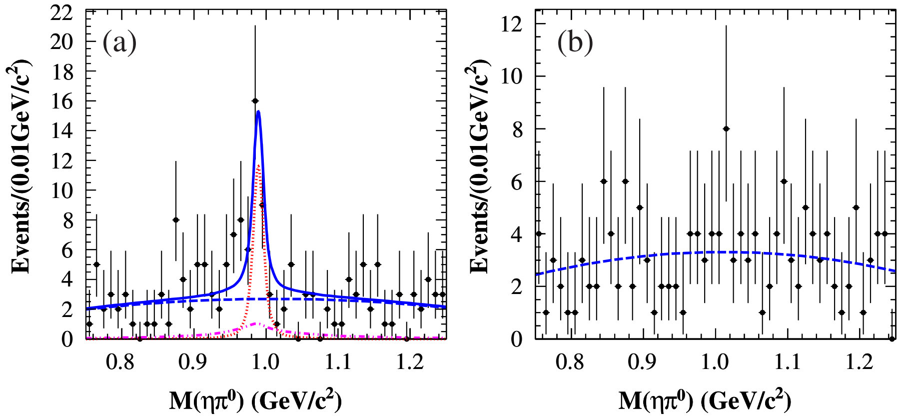

FIG. 2 (color online). Results of the simultaneous fit of the $\eta\pi^0$ mass spectra: (a) recoiling against the ϕ and (b) recoiling against the ϕ sideband. The solid curve in the result of the fit described in the text. The dotted curve is the mixing signal, and the dash-dotted curve is the $a_0^0(980)$ contribution from γ^* or K^*K loops. The dashed curves in (a) and (b) denote the background polynomial.

$$\mathrm{Br}\,(J/\psi \to \phi f_0(980) \to \phi a_0^0(980) \to \phi\eta\pi^0) = \frac{N(f_0 \to a_0^0)}{\varepsilon_{fa} \cdot N_{J/\psi} \cdot \mathrm{Br}(\phi \to K^+K^-) \cdot \mathrm{Br}(\eta \to \gamma\gamma) \cdot \mathrm{Br}(\pi^0 \to \gamma\gamma)},$$

where $N_{J/\psi}$ is the total number of J/ψ events and $\varepsilon_{fa} = (18.5 \pm 0.2)\%$ is the efficiency for the mixing signal $J/\psi \to \phi f_0(980) \to \phi a_0^0(980) \to \phi\eta\pi^0$. The branching ratio is then determined to be $(3.3 \pm 1.1) \times 10^{-6}$, where the error is statistical only.

The total branching ratio of $J/\psi \to \phi a_0^0(980) \to \phi\eta\pi^0$ is calculated as

$$\mathrm{Br}\,(J/\psi \to \phi\eta\pi^0) = \frac{N(f_0 \to a_0^0)/\varepsilon_{fa} + N(a_0^0)/\varepsilon_a}{N_{J/\psi} \cdot \mathrm{Br}(\phi \to K^+K^-) \cdot \mathrm{Br}(\eta \to \gamma\gamma) \cdot \mathrm{Br}(\pi^0 \to \gamma\gamma)},$$

where $\varepsilon_a = (18.3 \pm 0.2)\%$ is the efficiency for the underlying process $J/\psi \to \phi a_0^0(980) \to \phi\eta\pi^0$. The branching ratio is then determined to be $(5.0 \pm 2.7) \times 10^{-6}$, where the error is statistical only.

If we fit the $\eta\pi^0$ invariant mass spectrum only with the mixing signal plus a 2nd order polynomial background, the fit yields 28.6 ± 7.0 events for the mixing signal. Comparing with the fit result with only the 2nd order polynomial, the change in $-lnL$ with $\Delta(\mathrm{d.o.f.}) = 1$ is 16.65, corresponding to a statistical significance of 5.8σ. The upper limit at the 90% C.L. is 39.1 events.

If we assume there is no mixing and fit the $\eta\pi^0$ invariant mass spectrum only with the $a_0^0(980)$ contribution from γ^* or K^*K loops plus a 2nd order polynomial, the fit yields 75.8 ± 17.3 events for the $a_0^0(980)$ contribution from γ^* or K^*K loops. Comparing with the fit result with only the 2nd order polynomial, the change in $-lnL$ with $\Delta(\mathrm{d.o.f.}) = 1$ is 10.89, corresponding to a statistical significance of 4.7σ. The upper limit at the 90% C.L. is 99.1 events. The results are listed in Table I. The total branching ratio of $J/\psi \to \phi a_0^0(980) \to \phi\eta\pi^0$ is calculated to be $(9.7 \pm 2.2) \times 10^{-6}$, where the error is statistical only.

V. MEASUREMENT OF $\psi' \to \gamma\chi_{c1} \to \gamma\pi^0 a_0^0(980) \to \gamma\pi^0 f_0(980) \to \gamma\pi^0\pi^+\pi^-$

Events with two oppositely charged tracks identified as pions and at least three photons, which form at least one distinct π^0 candidate, are selected. A 5C kinematic fit is performed to the $\psi' \to \gamma\pi^0\pi^+\pi^-$ hypothesis (constraints are the 4-momentum of ψ' and the π^0 mass) and $\chi^2_{5C} < 60$ is required. If there is more than one combination, the

TABLE I. Results of fits to the mass spectrum of $\eta\pi^0$. The fit is described in the text, and the yield error is statistical only. $N(f_0 \to a_0^0)$ is the number of mixing events $f_0(980) \to a_0^0(980)$. $S(f_0 \to a_0^0)$ is the significance of the mixing signal $f_0(980) \to a_0^0(980)$. $N(a_0^0(980))$ is the number of $a_0^0(980)$ events from γ^* or K^*K loops. $S(a_0^0(980))$ is the significance of the $a_0^0(980)$ contribution from γ^* or K^*K loops.

Fitting with	$N(f_0 \to a_0^0)$	$S(f_0 \to a_0^0)$	$N(a_0^0(980))$	$S(a_0^0(980))$
mixing + $a_0^0(980)$ + 2nd poly	$25.8 \pm 8.6(<37.5)$	3.4σ	$13.6 \pm 24.8(<50.8)$	0.5σ
mixing + 2nd poly	$28.6 \pm 7.0(<39.1)$	5.8σ	$\cdots$	$\cdots$
$a_0^0(980)$ + 2nd poly	$\cdots$	$\cdots$	$75.8 \pm 17.3(<99.1)$	4.7σ

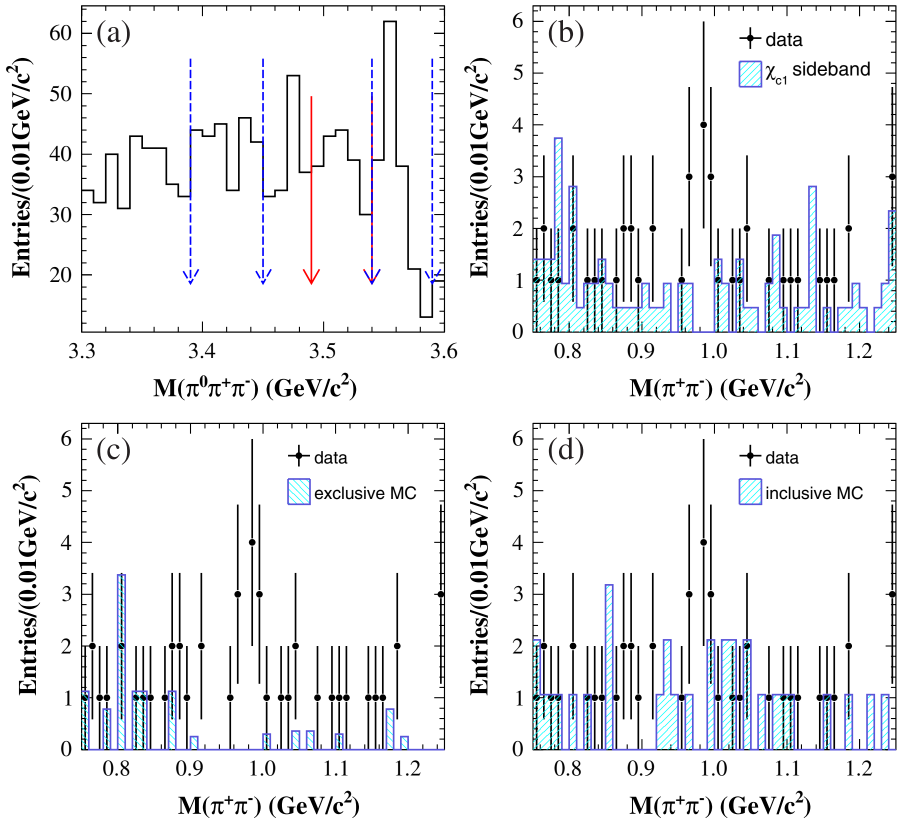

FIG. 3 (color online). (a) The invariant mass spectrum of $\pi^0\pi^+\pi^-$ in $\psi' \to \gamma\pi^+\pi^-\pi^0$. The solid arrows show the χ_{c1} mass window, and the dashed arrows show the χ_{c1} sideband region used to estimate background. The invariant mass of $\pi^+\pi^-$ of selected events is shown in (b)–(d). The dots with error bars show the mass spectrum of $M_{\pi^+\pi^-}$ in the χ_{c1} mass window. The shaded histogram is (b) χ_{c1} sideband; (c) from exclusive MC; and (d) from inclusive MC.

combination with the smallest χ^2_{5C} is retained. The events are also fitted to $\psi' \to \pi^0\pi^+\pi^-$ and $\psi' \to \pi^0\pi^0\pi^+\pi^-$, and the probabilities are required to be less than that from the kinematic fit to the signal channel $\psi' \to \gamma\pi^0\pi^+\pi^-$. To remove backgrounds with a J/ψ decaying to leptons, the angle between the two charged tracks is required to be less than 160°. We further require the ratio of energy deposited by each charged track in the EMC to its momentum measured in the main drift chamber to be less than 0.85. To remove the backgrounds which have $\gamma\gamma J/\psi$ final states, the mass recoiling from any photon pair must not be in the J/ψ mass window ($|M^{\gamma\gamma}_{\mathrm{recoiling}} - 3.097\ \mathrm{GeV}/c^2| > 0.06\ \mathrm{GeV}/c^2$). The invariant mass distribution of $\pi^0\pi^+\pi^-$ of the selected events is shown in Fig. 3(a).

The $\pi^+\pi^-$ invariant mass distribution in the χ_{c1} mass window ($3.49\ \mathrm{GeV}/c^2 < M_{\pi^0\pi^+\pi^-} < 3.54\ \mathrm{GeV}/c^2$) is shown in Fig. 3(b). A narrow structure around $980\ \mathrm{MeV}/c^2$ is evident. The shaded histogram shows the $\pi^+\pi^-$ invariant mass of events in the χ_{c1} sideband ($3.39\ \mathrm{GeV}/c^2 < M_{\pi^0\pi^+\pi^-} < 3.45\ \mathrm{GeV}/c^2$ and $3.54\ \mathrm{GeV}/c^2 < M_{\pi^0\pi^+\pi^-} < 3.59\ \mathrm{GeV}/c^2$).

Exclusive MC samples of ψ' decays which have similar final states are generated to check whether a peak near $980\ \mathrm{MeV}/c^2$ can be produced in the $\pi^+\pi^-$ mass spectrum. The main possible backgrounds come from: $\psi' \to \gamma\chi_{c1} \to \gamma\gamma J/\psi \to \gamma\gamma\pi^+\pi^-\pi^0$; $\psi' \to \pi^+\pi^-\pi^0$; $\psi' \to \gamma\chi_{c1} \to \gamma a_0^\pm(980)\pi^\mp \to \gamma\eta\pi^+\pi^-\pi^0$; and $\psi' \to \eta\pi^+\pi^-\pi^0$. The $\pi^+\pi^-$ invariant mass distributions from all these background channels is shown as the shaded histogram in Fig. 3(c), and there is no peak around $980\ \mathrm{MeV}/c^2$.

A MC sample of 1.0×10^8 inclusive ψ' decay events is used to investigate other possible backgrounds. The shaded area in Fig. 3(d) shows the $\pi^+\pi^-$ invariant mass distribution of events selected from the inclusive MC sample. In the $980\ \mathrm{MeV}/c^2$ region, there is no peaking background. The $f_0(980)$ from other $\psi' \to \gamma\chi_{c1} \to \gamma\pi^0 f_0(980)$ processes is much broader than the $a_0^0(980) \to f_0(980)$ mixing signal [14] and is estimated from the fit.

A simultaneous fit is performed to the $\pi^+\pi^-$ invariant mass spectrum in the χ_{c1} mass window and the χ_{c1} sideband in a similar manner as in Sec. IV. The $f_0(980)$ contribution from other processes is represented by a Flatté formula.[2] Figures 4(a) and 4(b) show the results of the simultaneous fit.

[2]The Flatté formula is quoted from Ref. [18]. The values of coupling constants and mass used here are quoted from BES II experiment results [14,20].

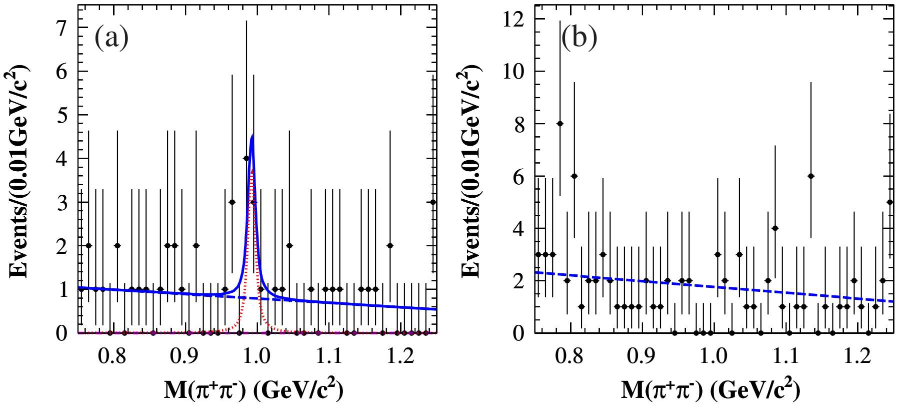

FIG. 4 (color online). Results of the simultaneous fit of the $\pi^+\pi^-$ mass spectra: (a) in the χ_{c1} mass window and (b) in the χ_{c1} sideband region. The solid curve is the result of fit described in the text. The dotted curve shows the mixing signal. The dash-dotted curve indicates $f_0(980)$ from other processes. The dashed curves in (a) and (b) denote the background polynomial.

The fit yields $N(a_0^0 \to f_0) = 6.4 \pm 3.2$ events for the mixing signal and $N(f_0(980)) = 0.0 \pm 8.6$ events for the $f_0(980)$ contribution from other processes. Comparing with the fit result without the mixing signal, the change in $-lnL$ with $\Delta(\text{d.o.f.}) = 1$ is 1.79, corresponding to a statistical significance of 1.9σ. Comparing with the fit result without the $f_0(980)$ contribution from other processes, the change in $-lnL$ with $\Delta(\text{d.o.f.}) = 1$ is less than 0.01, corresponding to a statistical significance of less than 0.1σ. Using the Bayesian method, the upper limit for the number of the mixing events is 11.9, and the upper limit for the number of the $f_0(980)$ events from other processes is 16.7 events at the 90% C.L. The results are listed in Table II.

The branching ratio of the mixing signal $\psi' \to \gamma\chi_{c1} \to \gamma\pi^0 a_0^0(980) \to \gamma\pi^0 f_0(980) \to \gamma\pi^0\pi^+\pi^-$ is calculated as

$$\mathrm{Br}\,(\psi' \to \gamma\chi_{c1} \to \gamma\pi^0 a_0^0(980) \to \gamma\pi^0 f_0(980) \to \gamma\pi^0\pi^+\pi^-) = \frac{N(a_0^0 \to f_0)}{\varepsilon_{af} \cdot N_{\psi'} \cdot \mathrm{Br}(\pi^0 \to \gamma\gamma)},$$

where $N_{\psi'}$ is the total number of ψ' events and $\varepsilon_{af} = (22.3 \pm 0.2)\%$ is the efficiency for the mixing signal $\psi' \to \gamma\chi_{c1} \to \gamma\pi^0 a_0^0(980) \to \gamma\pi^0 f_0(980) \to \gamma\pi^0\pi^+\pi^-$. The branching ratio is then determined to be $(2.7 \pm 1.4) \times 10^{-7}$, where the error is statistical only.

The total branching ratio of $\psi' \to \gamma\chi_{c1} \to \gamma\pi^0\pi^+\pi^-$ is calculated as

$$\mathrm{Br}\,(\psi' \to \gamma\chi_{c1} \to \gamma\pi^0 a_0^0(980) \to \gamma\pi^0 f_0(980) \to \gamma\pi^0\pi^+\pi^-) = \frac{N(a_0^0 \to f_0)/\varepsilon_{af} + N(f_0)/\varepsilon_f}{N_{\psi'} \cdot \mathrm{Br}(\pi^0 \to \gamma\gamma)},$$

where $\varepsilon_f = (20.5 \pm 0.2)\%$ is the efficiency for the underlying process $\psi' \to \gamma\pi^0 f_0(980) \to \gamma\pi^0\pi^+\pi^-$. The branching ratio is then determined to be $(2.7 \pm 4.2) \times 10^{-7}$, where the error is statistical only.

If we fit the $\pi^+\pi^-$ invariant mass spectrum only with the mixing signal plus a 2nd order polynomial background, the fit yields 6.4 ± 3.2 events for the mixing signal. Comparing with the fit result with only the 2nd order polynomial, the change in $-lnL$ with $\Delta(\text{d.o.f.}) = 1$ is 4.41, corresponding to a statistical significance of 3.0σ. The upper limit at the 90% C.L. is 12.1 events.

If we assume there is no mixing and fit the $\pi^+\pi^-$ invariant mass spectrum only with the $f_0(980)$ contribution from other processes plus a 2nd order polynomial, the fit yields 12.8 ± 6.7 events for the $f_0(980)$ contribution from other processes. Comparing with the fit result with only the 2nd order polynomial, the change in $-lnL$ with $\Delta(\text{d.o.f.}) = 1$ is 2.62, corresponding to a statistical significance of 2.3σ. The upper limit at the 90% C.L. is 23.6 events. The fit results are listed in Table II. The total branching ratio of $\psi' \to \gamma\chi_{c1} \to \gamma\pi^0 f_0(980) \to \gamma\pi^0\pi^+\pi^-$ is calculated to be $(6.0 \pm 3.1) \times 10^{-7}$, where the error is statistical only.

TABLE II. Results of fits to the $\pi^+\pi^-$ invariant mass spectrum in the χ_{c1} region. The fit is described in the text, and the yield error is only statistical. $N(a_0^0 \to f_0)$ is the number of mixing events $a_0^0(980) \to f_0(980)$. $S(a_0^0 \to f_0)$ is the significance of the mixing signal $a_0^0(980) \to f_0(980)$. $N(f_0(980))$ is the number of $f_0(980)$ events from other processes. $S(f_0(980))$ is the significance of the $f_0(980)$ contribution from other processes.

Mode	$N(a_0^0 \to f_0)$	$S(a_0^0 \to f_0)$	$N(f_0(980))$	$S(f_0(980))$
mixing + $f_0(980)$ + 2nd poly	$6.4 \pm 3.2(<11.9)$	1.9σ	$0.0 \pm 8.6(<16.7)$	$<0.1\sigma$
mixing + 2nd poly	$6.4 \pm 3.2(<12.1)$	3.0σ	$\cdots$	$\cdots$
$f_0(980)$ + 2nd poly	$\cdots$	$\cdots$	$12.8 \pm 6.7(<23.6)$	2.3σ

TABLE III. Fitting results with various theoretical and experimental values of the resonance parameters.

Mixing shape	$N(f_0 \to a_0^0)$	$S(f_0 \to a_0^0)$	$N(a_0^0 \to f_0)$	$S(a_0^0 \to f_0)$
$q\bar{q}$ [2]	$19.8 \pm 8.6(<31.8)$	2.4σ	$5.9 \pm 2.8(<10.9)$	2.0σ
$q^2\bar{q}^2$ [2]	$19.4 \pm 8.5(<31.5)$	2.4σ	$6.3 \pm 3.0(<11.5)$	2.1σ
$K\bar{K}$ [3–5]	$14.5 \pm 10.8(<28.3)$	1.3σ	$5.8 \pm 2.7(<10.5)$	1.6σ
$q\bar{q}g$ [6]	$25.4 \pm 9.7(<38.2)$	2.9σ	$6.6 \pm 3.2(<12.2)$	2.6σ
SND [21,22]	$21.7 \pm 9.3(<33.1)$	2.5σ	$6.0 \pm 2.9(<11.1)$	2.0σ
KLOE [23,24]	$23.3 \pm 8.0(<34.9)$	3.3σ	$6.3 \pm 3.0(<11.6)$	2.0σ
BNL [25]	$28.7 \pm 6.8(<38.7)$	4.1σ	$6.4 \pm 3.0(<11.8)$	2.4σ
CB [19]	$27.1 \pm 8.4(<37.8)$	3.7σ	$6.4 \pm 3.1(<11.8)$	2.2σ

VI. DISCUSSION

Various models for the $a_0^0(980)$ and the $f_0(980)$ [2–6] give different predictions for their coupling constants and masses; these have been measured by several experiments [19,21–25]. From these theoretical and experimental values of the resonance parameters, predictions for ξ_{af} and ξ_{fa} are calculated [13,14]. Using the parameter sets listed in Table III, the line shapes of the $a_0^0(980) \to f_0(980)$ and $f_0(980) \to a_0^0(980)$ mixing signals can be determined from MC simulation, and the underlying $f_0(980)$ ($a_0^0(980)$) shapes can be parameterized accordingly. Table III shows the fitting results obtained using a similar fitting procedure as described in Secs. IV and V. The fitting results are consistent within the statistical error.

VII. SYSTEMATIC UNCERTAINTIES

The systematic uncertainties on the branching ratios are summarized in Table IV.

The systematic uncertainty associated with the tracking efficiency has been studied with control samples such as $J/\psi \to \rho\pi$, $J/\psi \to p\bar{p}\pi^+\pi^-$, and $J/\psi \to K^*K \to K_SK\pi$. The difference of the tracking efficiencies between data and MC simulation is 2% per charged track.

The uncertainties due to PID of π and K are determined from studies of control samples such as $J/\psi \to \rho\pi$, $J/\psi \to p\bar{p}\pi^+\pi^-$, and $J/\psi \to K^*K \to K^+K^-\pi^0$. The difference of the PID efficiency between data and MC is 2% per track.

TABLE IV. Summary of systematic errors for the branching ratio measurements and upper limits determination.

$J/\psi \to \phi a_0^0(980) \to \phi\eta\pi^0$	Mixing Br	Upper limit of mixing Br	Total Br	Total Br (no mixing)
Charged tracks	4.0%	4.0%	4.0%	4.0%
Photon detection	4.0%	4.0%	4.0%	4.0%
PID	4.0%	4.0%	4.0%	4.0%
η construction	2.0%	2.0%	2.0%	2.0%
π^0 construction	2.0%	2.0%	2.0%	2.0%
Kinematic fit	0.9%	0.9%	0.9%	0.9%
Intermediate decay	0.54%	0.54%	0.54%	0.54%
Normalization	1.3%	1.3%	1.3%	1.3%
Background shape	6.6%	⋯	28.7%	4.9%
Fitting range	6.2%	⋯	14.5%	12.9%
Total	11.9%	7.7%	33.1%	15.8
$\psi' \to \gamma\chi_{c1} \to \gamma\pi^0 f_0(980) \to \gamma\pi^0\pi^+\pi^-$				
Charged tracks	4.0%	4.0%	4.0%	4.0%
Photon detection	3.0%	3.0%	3.0%	3.0%
PID	4.0%	4.0%	4.0%	4.0%
π^0 construction	2.0%	2.0%	2.0%	2.0%
Kinematic fit	1.7%	1.7%	1.7%	1.7%
Intermediate decay	0.034%	0.034%	0.034%	0.034%
Normalization	4.0%	4.0%	4.0%	4.0%
Background shape	23.4%	⋯	128.1%	48.4%
Fitting range	6.3%	⋯	32.8%	17.2%
Total	25.5%	8.0%	132.5%	52.0%

The uncertainty due to photon detection and photon conversion is 1% per photon. This is determined from studies of the photon detection efficiency in control samples such as $J/\psi \to \rho^0\pi^0$ and a study of photon conversion via $e^+e^- \to \gamma\gamma$.

The uncertainty due to the π^0 selection is determined from a high purity control sample of $J/\psi \to \pi^+\pi^-\pi^0$ decays. The π^0 selection efficiency is obtained from the change in the π^0 yield in the $\pi^+\pi^-$ recoiling mass spectrum with or without the π^0 selection requirement. The difference of the π^0 reconstruction efficiency between data and MC simulation gives an uncertainty of 2.0% per π^0. The uncertainty from the η selection is 2.0% per η, which is determined in a similar way from a control sample of $J/\psi \to p\bar{p}\eta$.

The uncertainty of the kinematic fit for $J/\psi \to \phi f_0(980) \to \phi a_0^0(980) \to \phi\eta\pi^0$ is estimated from $J/\psi \to \omega\eta \to \pi^+\pi^-\pi^0\eta$ ($\eta, \pi^0 \to \gamma\gamma$). The efficiency is obtained from the change in the yield of ω signal by a fit to the $\pi^+\pi^-\pi^0$ mass distribution with or without the requirement of the kinematic fit. The systematic uncertainty is determined to be 0.9%. The uncertainty of the kinematic fit for $\psi' \to \gamma\chi_{c1} \to \gamma\pi^0 a_0^0(980) \to \gamma\pi^0 f_0(980) \to \gamma\pi^0\pi^+\pi^-$ is estimated to be 1.7% from $\psi' \to \pi^+\pi^- J/\psi$, $J/\psi \to \gamma\eta$.

The branching ratios for the $\eta \to \gamma\gamma$, $\pi^0 \to \gamma\gamma$, and $\phi \to K^+K^-$ decays are taken from the Particle Data Group [17]. The uncertainty on these branching ratios is taken as a systematic uncertainty in our measurements.

The total number of J/ψ events is $(2.252 \pm 0.028) \times 10^8$, determined from inclusive J/ψ hadronic decays [15], and the total number of ψ' events is $(1.06 \pm 0.04) \times 10^8$, determined from inclusive ψ' hadronic events [16]. The uncertainty on the number of J/ψ events is 1.3%, and the uncertainty on the number of ψ' events is 4%.

To estimate the systematic uncertainties due to the fit procedure, we repeat the fit with appropriate modifications to estimate the systematic uncertainties. The largest difference of the yield of each sources with respect to the values derived from the standard fit is considered as a systematic error. We change the sideband range and the order of the polynomial to estimate the uncertainty from the background shape. A series of fits using different fitting ranges is performed and the largest change of the branching ratios is assigned as a systematic uncertainty.

The total systematic uncertainties for the branching ratio measurements are obtained by adding up the contributions from all the systematic sources in quadrature.

The uncertainty due to the parameterization of the mixing signal line shape and the underlying $a_0^0(980)$ [$f_0(980)$] is kept separate and quoted as a second systematic uncertainty. The uncertainty is obtained by comparing the results with the parameter sets in Table III with the standard fit. We take this difference as a conservative estimate of the uncertainty and assign an uncertainty of 43.8% for the $a_0^0(980) \to f_0(980)$ mixing measurement and an uncertainty of 9.4% for the $f_0(980) \to a_0^0(980)$ mixing measurement. For the total branching ratio measurement of $J/\psi \to \phi a_0^0(980) \to \phi\eta\pi^0$, the uncertainty is assigned to be 38.3%, and for the total branching ratio measurement of $\psi' \to \gamma\chi_{c1} \to \gamma\pi^0 f_0(980) \to \gamma\pi^0\pi^+\pi^-$, the uncertainty is assigned to be 9.4%. If we assume there is no mixing, the uncertainties of the total branching ratio measurements are assigned to be 41.4% and 42.2%, respectively.

VIII. SUMMARY

Based on $(2.252 \pm 0.028) \times 10^8 J/\psi$ events and $(1.06 \pm 0.04) \times 10^8 \psi'$ events, the mixing branching ratios are measured to be $\mathrm{Br}(J/\psi \to \phi f_0(980) \to \phi a_0^0(980) \to \phi\eta\pi^0) = (3.3 \pm 1.1(\mathrm{stat}) \pm 0.4(\mathrm{sys}) \pm 1.4(\mathrm{para})) \times 10^{-6}$, $\mathrm{Br}(\psi' \to \gamma\chi_{c1} \to \gamma\pi^0 a_0^0(980) \to \gamma\pi^0 f_0(980) \to \gamma\pi^0\pi^+\pi^-) = (2.7 \pm 1.4(\mathrm{stat}) \pm 0.7(\mathrm{sys}) \pm 0.3(\mathrm{para})) \times 10^{-7}$, where the uncertainties are statistical, systematics due to this measurement, and systematics due to the parameterization, respectively.

The total branching ratio of $J/\psi \to \phi a_0^0(980) \to \phi\eta\pi^0$ is measured to be $(5.0 \pm 2.7(\mathrm{stat}) \pm 1.7(\mathrm{sys}) \pm 1.9(\mathrm{para})) \times 10^{-6}$, and the total branching ratio of $\psi' \to \gamma\chi_{c1} \to \gamma\pi^0 f_0(980) \to \gamma\pi^0\pi^+\pi^-$ is measured to be $(2.7 \pm 4.2(\mathrm{stat}) \pm 3.6(\mathrm{sys}) \pm 0.3(\mathrm{para})) \times 10^{-7}$. If we assume there is no mixing, the total branching ratios are measured to be $(9.7 \pm 2.2(\mathrm{stat}) \pm 1.5(\mathrm{sys}) \pm 4.0(\mathrm{para})) \times 10^{-6}$ and $(6.0 \pm 3.1(\mathrm{stat}) \pm 3.1(\mathrm{sys}) \pm 2.5(\mathrm{para})) \times 10^{-7}$, respectively.

When determining the upper limit of the number of $J/\psi \to \phi f_0(980) \to \phi a_0^0(980) \to \phi\eta\pi^0$ events, the uncertainties due to the fit range, background shape, the parameterization of mixing signal line shape, and the underlying $a_0^0(980)$ are considered. Using the Bayesian method, different upper limits at the 90% C.L. are determined by varying the fit range, the background shape and the parameterization of the mixing signal line shape, and the underlying $a_0^0(980)$ in Table III. The upper limit for the mixing signal is taken to be the largest of them: $N_{fa}^{\mathrm{U.L.}} = 39.7$ events. A conservative estimate of the upper limit of the branching ratio is determined by lowering the efficiency by 1 standard deviation.

The upper limit on the branching ratio at the 90% C.L. is calculated as

$$\mathrm{Br}(J/\psi \to \phi f_0(980) \to \phi a_0^0(980) \to \phi\eta\pi^0) < \frac{N_{fa}^{\mathrm{U.L.}}}{(\varepsilon_{fa} - \sigma_{fa}^{\mathrm{U.L.}}) \cdot N_{J/\psi} \cdot \mathrm{Br}(\phi \to K^+K^-) \cdot \mathrm{Br}(\eta \to \gamma\gamma) \cdot \mathrm{Br}(\pi^0 \to \gamma\gamma)} = 5.4 \times 10^{-6}.$$

Similarly, considering the uncertainties due to fit range, background shape, the parameterization of mixing signal line shape, and the underlying $f_0(980)$, the upper limit number of the mixing signal $\psi' \to \gamma\chi_{c1} \to \gamma\pi^0 a_0^0(980) \to \gamma\pi^0 f_0(980) \to \gamma\pi^0\pi^+\pi^-$ is determined to be $N_{af}^{\text{U.L.}} = 13.0$ events.

The upper limit on the branching ratio at the 90% C.L. is calculated as

$$\begin{aligned}\mathrm{Br}(&\psi' \to \gamma\chi_{c1} \to \gamma\pi^0 a_0^0(980) \to \gamma\pi^0 f_0(980) \\ &\to \gamma\pi^0\pi^+\pi^-) < \frac{N_{af}^{\text{U.L.}}}{(\varepsilon_{af} - \sigma_{af}^{\text{U.L.}}) \cdot N_{\psi'} \cdot \mathrm{Br}(\pi^0 \to \gamma\gamma)} \\ &= 6.0 \times 10^{-7}.\end{aligned}$$

The mixing intensity ξ_{fa} for the $f_0(980) \to a_0^0(980)$ transition is calculated to be

$$\begin{aligned}\xi_{fa} &= \frac{\mathrm{Br}(J/\psi \to \phi f_0(980) \to \phi a_0^0(980) \to \phi\eta\pi^0)}{\mathrm{Br}(J/\psi \to \phi f_0(980) \to \phi\pi\pi)^{[20]}} \\ &= (0.60 \pm 0.20(\text{stat})) \pm 0.12(\text{sys}) \pm 0.26(\text{para})\%,\end{aligned}$$

where the uncertainties are statistical, systematics due to this measurement, and the parameterization, respectively. The uncertainty from $\mathrm{Br}(J/\psi \to \phi f_0(980) \to \phi\pi\pi)$ is included as a part of the systematic error. The upper limit of the mixing intensity ξ_{fa} at the 90% C.L. is 1.1%.

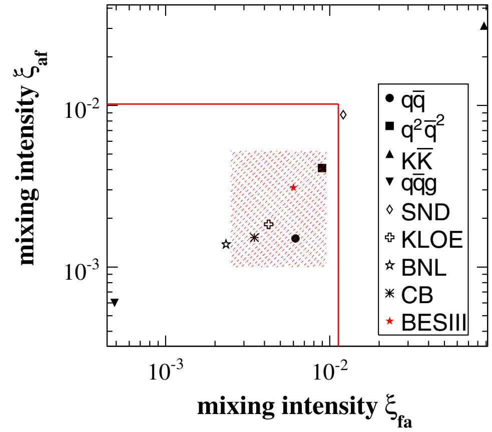

FIG. 5 (color online). Mixing intensities of $f_0(980) \to a_0^0(980)$ and $a_0^0(980) \to f_0(980)$. The dots are predictions for the mixing intensities with theoretical and experimental values of the parameters [14]. The shaded region is our results with statistical errors and systematics due to this measurement and the parameterization. The solid lines mark the upper limits.

The mixing intensity ξ_{af} for the $a_0^0(980) \to f_0(980)$ transition is calculated to be

$$\xi_{af} = \frac{\mathrm{Br}(\psi' \to \gamma\chi_{c1} \to \gamma\pi^0 a_0^0(980) \to \gamma\pi^0 f_0(980) \to \gamma\pi^0\pi^+\pi^-)}{\mathrm{Br}(\psi' \to \gamma\chi_{c1} \to \gamma\pi^0 a_0^0(980) \to \gamma\pi^0\pi^0\eta)^{[17]}} = (0.31 \pm 0.16(\text{stat}) \pm 0.14(\text{sys}) \pm 0.03(\text{para}))\%.$$

The uncertainty from $\mathrm{Br}(\psi' \to \gamma\chi_{c1} \to \gamma\pi^0 a_0^0(980) \to \gamma\pi^0\pi^0\eta)$ is included as a part of the systematic error. The upper limit of the mixing intensity ξ_{af} at the 90% C.L. is 1.0%.

The calculated mixing intensities [14] with the resonance parameters from various models [2–6] and experimental measurements [19,21–25] are compared with our results in Fig. 5. This result will be very useful in pinning down the resonance parameters of $a_0^0(980)$ and $f_0(980)$.

ACKNOWLEDGMENTS

The BES III Collaboration thanks the staff of BEPC II and the computing center for their hard efforts. This work is supported in part by the Ministry of Science and Technology of China under Contract No. 2009CB825200; National Natural Science Foundation of China (NSFC) under Contracts No. 10625524, No. 10821063, No. 10825524, No. 10835001, No. 10875113, No. 10935007, No. 10979008, No. 10979038, No. 11005109, and No. 11079030; the Chinese Academy of Sciences (CAS) Large-Scale Scientific Facility Program; CAS under Contracts No. KJCX2-YW-N29 and No. KJCX2-YW-N45; 100 Talents Program of CAS; Research Fund for the Doctoral Program of Higher Education of China under Contract No. 20093402120022; Istituto Nazionale di Fisica Nucleare, Italy; Russian Foundation for Basic Research under Contracts No. 08-02-92221 and No. 08-02-92200-NSFC-a; Siberian Branch of Russian Academy of Science, joint project No. 32 with CAS; U.S. Department of Energy under Contracts No. DE-FG02-04ER41291, No. DE-FG02-91ER40682, and No. DE-FG02-94ER40823; University of Groningen (RuG) and the Helmholtzzentrum fuer Schwerionenforschung GmbH (GSI), Darmstadt; and WCU Program of National Research Foundation of Korea under Contract No. R32-2008-000-10155-0.

[1] R. L. Jaffe, Phys. Rev. D **15**, 267 (1977).
[2] N. N. Achasov and V. N. Ivanchenko, Nucl. Phys. **B315**, 465 (1989).
[3] N. N. Achasov and V. V. Gubin, Phys. Rev. D **56**, 4084 (1997).
[4] J. D. Weinstein and N. Isgur, Phys. Rev. D **27**, 588 (1983).
[5] J. D. Weinstein and N. Isgur, Phys. Rev. D **41**, 2236 (1990).
[6] S. Ishida *et al.*, in *Proceedings of the 6th International Conference on Hadron Spectroscopy, Manchester, United Kingdom, 1995* (World Scientific, Singapore, 1995), p. 454.
[7] N. N. Achasov, S. A. Devyanin, and G. N. Shestakov, Phys. Lett. **88B**, 367 (1979).
[8] C. Hanhart, B. Kubis, and J. R. Pelaez, Phys. Rev. D **76**, 074028 (2007).
[9] N. N. Achasov and A. V. Kiselev, Phys. Lett. B **534**, 83 (2002).
[10] B. Kerbikov and F. Tabakin, Phys. Rev. C **62**, 064601 (2000).
[11] N. N. Achasov and G. N. Shestakov, Phys. Rev. Lett. **92**, 182001 (2004).
[12] F. E. Close and A. Kirk, Phys. Lett. B **489**, 24 (2000).
[13] J. J. Wu, Q. Zhao, and B. S. Zou, Phys. Rev. D **75**, 114012 (2007).
[14] J. J. Wu and B. S. Zou, Phys. Rev. D **78**, 074017 (2008).
[15] M. Ablikim *et al.* (BES III Collaboration), Phys. Rev. D, **83**, 012003 (2011).
[16] M. Ablikim *et al.*, Phys. Rev. D **81**, 052005 (2010).
[17] K. Nakamura *et al.* (Particle Data Group), J. Phys. G **37**, 075021 (2010).
[18] S. M. Flatte, Phys. Lett. **63B**, 224 (1976).
[19] D. V. Bugg, V. V. Anisovich, A. Sarantsev, and B. S. Zou, Phys. Rev. D **50**, 4412 (1994).
[20] M. Ablikim *et al.* (BES Collaboration), Phys. Lett. B **607**, 243 (2005).
[21] M. N. Achasov *et al.*, Phys. Lett. B **485**, 349 (2000).
[22] M. N. Achasov *et al.*, Phys. Lett. B **479**, 53 (2000).
[23] A. Aloisio *et al.* (KLOE Collaboration), Phys. Lett. B **536**, 209 (2002).
[24] A. Aloisio *et al.* (KLOE Collaboration), Phys. Lett. B **537**, 21 (2002).
[25] S. Teige *et al.* (E852 Collaboration), Phys. Rev. D **59**, 012001 (1998).